

# Automatic Compensation of the Positional Error Utilizing Localization Method in Pipe

Hirofumi Maeda



**Abstract:** Since 1965, a numerous number of cities implementing sewerage systems have increased rapidly throughout Japan, and sewerage development is considered to be becoming more widespread in various regions. However, with the increase of management facilities, the aging of facilities for long-term use is becoming more and more apparent. The standard expected durability of these pipes is approximately 50 years, but there is a tendency and a risk that the number of collapsed roads will increase rapidly 30 years after the pipes are laid. Against this background, maintenance of drainage and sewage pipes is critical and must be carried out continuously. Therefore, in recent years, investigation using robots have been actively conducted in order to reduce manual workload of the workers. However, these robots have a large-scale system as a whole, and as a result, they are poorly maintainable and expensive. Therefore, in this research, I have developed an autonomous and portable pipe inspection robot through the know-how on rescue robots which I have studied so far. However, for inspections using a pipe inspection robot, there is always the risk that the robot itself will tip over due to steps or small gaps at the joints of the pipes or slips caused by sludge. Therefore, to prevent tumbles and rollovers of the robot, I propose a localization method only by straight-driving control without relying on hardware. In addition, taking possible slips inside pipes into account, this method utilizes only acceleration sensor. In this study, localization method using only accelerometer mounted on the robot, which focuses on the relation between the pipe and the contact point of the tires, was shown as well as presenting a method using numerical analysis to derive the estimated values. Furthermore, it was confirmed that the estimation was stable as a result of an estimation experiment using autonomous small pipe inspection robot with and without a gradient (approx. 4/100) of a pipe, with a diameter of 189mm.

**Keywords:** Exploration Robot, Mobile Robot, Water Pipe, Localization, Robot Control

## I. INTRODUCTION

Since 1965, a numerous number of cities implementing sewerage systems have increased rapidly throughout Japan, and sewerage development is considered to be becoming more widespread in various regions. So far, the total length of sewerage pipes is approx. 460,000 km, and the number of sewage treatment facilities is approx. 2,200. For that reason, with the increase of management facilities, the aging of facilities for long-term use is becoming more and more apparent.

Manuscript received on January 10, 2021.

Revised Manuscript received on January 20, 2021.

Manuscript published on January 30, 2021.

\* Correspondence Author

**Hirofumi Maeda\***, Department of Information Science and Technology, National Institute of Technology (KOSEN), Yuge College, Ehime Prefecture, Japan. Email: maeda@info.yuge.ac.jp

© The Authors. Published by Blue Eyes Intelligence Engineering and Sciences Publication (BEIESP). This is an [open access](https://creativecommons.org/licenses/by-nc-nd/4.0/) article under the CC BY-NC-ND license (<http://creativecommons.org/licenses/by-nc-nd/4.0/>)

The standard expected durability of these pipes is approximately 50 years, but the length of these drainage pipes beyond this number of durability years is approx. 10,000 km

or more. Moreover, there is a tendency and a risk that the number of collapsed roads will increase rapidly 30 years after the pipes are laid. However, the actual in-pipe inspection is harsh for workers and also the range of inspection is vast. In line with this, recently, robots have been actively used for inspection [1]. Typical pipe inspection robots currently in use are IBAK Panorama, DigiSewer iPEK, and RICO RPP. For Japanese-made robots, Toshiba Teli VCM561L, Hokuryo Co., Ltd. Mini-mogu, and QI TKC-3900, etc. These pipe inspection robots are self-propelled vehicles and only the robot body, which is physically connected to the control system on the transport vehicle placed near the manhole, is put into the pipe. By doing so, not only can the robot itself be lighter by placing the control unit and power supply unit on the ground, but also enables remote control with cables, making it possible to respond to unforeseen circumstances with high reliability. However, on the other hand, there are cases where it is necessary to close the roads in order to place the transport vehicles with control units on the ground, or multiple workers are required for inspection. In addition, the whole system requires large scale operation in terms of human resources and related physical requirement, and as such, its running cost is fairly expensive. Therefore, the method that is currently becoming the mainstream in this field is the stand-alone operation of the robot. This type of operation makes the operation inexpensive because the robot can be lighter, easier to carry compared to the old generation operation, and also makes it possible to operate by a small number of workers with a great feature that multiple pipes can be inspected at the same time. Outside Japan, MAKRO and MAIRO are famous on the research level [2]-[4], and Solo Robots of RedZone Robotics Inc. is famous on the production level, but since the standard pipe diameter outside Japan is 200 mm or more, these robots cannot be used for pipes with the diameter of 150 mm, which is the standard in Japan. KANTARO, which was developed by Kitakyushu Foundation for the Advancement of Industry, Science and Technology (FAIS) [5]-[8], is a Japanese-made pipe inspection robot aimed at complete autonomy, and it has a unique mechanism called inverted v shaped crawler, and can be operated for a wide range of diameters from 150 mm to 250 mm. Furthermore, KANTARO was productized as Mogurinko series by Ishikawa Iron Works Co., Ltd.

## Automatic Compensation of the Positional Error Utilizing Localization Method in Pipe

Mogurinko series were realized at low cost by omitting the autonomous feature from KANTARO, and also realizes autonomous-driving screening inspection by a single robot (stand-alone type) at the production level. However, there are still few kinds of stand-alone type robots both in Japan and overseas despite the contribution they can make.

Therefore, it is critical to implement miniaturized sensors, which have been rapidly developed in recent years, on pipe inspection robots, aiming to realize various autonomous controls and reduce workloads for workers more than ever. In this study, the ideas of the rescue robot [9]-[11] which we have been developing over a long period were applied to develop a small, portable inspection robot for screening inspection (video recording only) [12]-[16] is proposed inspired by the “secret box”, which is one of the traditional Japanese crafts “Hakone wooden mosaic work.”

Apart from this, for inspections using a pipe inspection robot, there is always the risk that the robot itself will tip over due to steps or cave-ins at the joints of the pipes or slips caused by sludge. In remote control with cables, the operator constantly grasps the position and the posture of the robot through the monitor, making it possible to prevent tumbles or rollovers. On the other hand, stand-alone pipe inspection robot needs to be equipped with control system on them to prevent them because it needs to perform all the inspection process autonomously by itself. For this reason, most of the stand-alone types so far have been able to prevent falls by adjusting the size of the robot to the target pipe diameter by replacing tires or in similar ways. The pipe inspection robot we developed works almost the same way by changing tires, and simple straight-driving control using an acceleration sensor was only auxiliary. However, relying on changing hardware not only leads to wasting time for preparation before and after inspection, but also has the risk of resulting in causing damages or losing parts of the robot. Also, tools have to be carried with the robot, making it even more expensive. Therefore, aside from relying on hardware, I propose implementing highly accurate straight-driving control (fall suppression). It is vital to develop highly accurate localization to realize this control using a gyro sensor. However as mentioned earlier, considering steps or gaps at the joint of the pipe or possible slip caused by sludge, relying solely on the gyro sensor is not necessarily reliable. Therefore, it would be possible to prevent slippage (slip correction) or reset (zero position correction) its coordinates if localization in absolute coordinates is realized by using only accelerometer. In this paper, we first outline the autonomous small pipe inspection robot utilizing the method above, followed by describing the method using only the acceleration sensor based on the estimation conditions. Finally, the estimation results from the experiments conducted using the actual machine are discussed in order to show the effectiveness of the estimation method.

## II. PROBLEM DEFINITION AND PIPE INSPECTION ROBOT

The major problem is the robot rolling over when inspection. If there is a large difference between the angles of traveling direction of the robot (initial posture) when it is set inside the pipe and the direction of pipe installation, robot can roll over even if its posture is maintained by the gyro sensor.

Especially when the pipe diameter is small, the effect of this difference becomes apparent. Apart from this, there is a possibility that the robot body will tip over (sensor value will drift) due to step difference at the pipe joint, gaps between pipes, slips caused by sludge.

Therefore, in order to solve these problems, I propose robot localization method by using only an accelerometer, enabling to detect the direction of gravitational acceleration when the robot is static (when acceleration by the robot is not generated) and to estimate the initial posture of the robot in the pipe to correct the posture when slipping. In addition, even when the robot is performing a linear uniform motion, acceleration by the driving unit on the robot itself does not occur, which can be used for localization.

For the research, small pipe inspection robot was used to show effectiveness of the localization method (Figure 1).



Fig. 1 Small Autonomous Pipe Inspection Robot

The size of the robot is 329.0 mm (W) x 132.6 mm (D) x 107.0 mm (H), and the weight of the main body is approx. 4.8 kg. The center of gravity is in front of the center of its main body. In addition, the tires are compatible with pipes with a diameter of 150 mm, and it can also be used for pipes with a diameter of 200 mm by attaching an additional tire unit. However, in this study, the additional tire unit was not attached to examine the localization accuracy by intentionally tilting the robot. Finally, Figure 2 shows the dimensions of the robot.

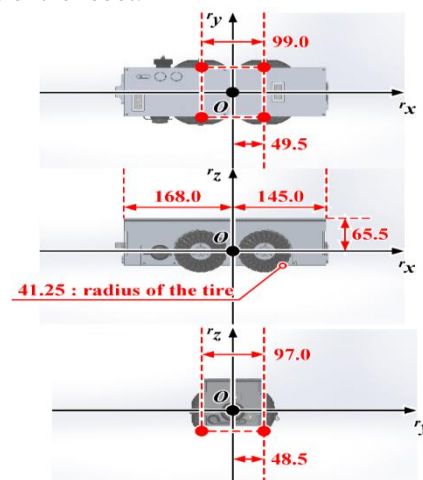


Fig. 2 Dimensions Required for Localization



### III. PROPOSAL OF LOCALIZATION IN PIPES

#### A. Estimation Conditions

I propose localization method under the following two conditions.

##### 1. Vibration is not considered

The robot is equipped with four tires, and three of them touch the ground when it is static in a columnar pipe (when the robot faces directly in front of the direction of travel, four tires touch the ground). But when the robot receives a strong impact, the robot vibrates with two diagonal tires touching the ground being the base point. However, in addition to the fact that this phenomenon is rare, since the center of gravity of the robot is in front, the vibration will soon subside.

##### 2. The contact point with the pipe is always directly underneath the tires

For all three (or four) tires, the contact points between the pipe and the tires are set to the part directly underneath the tires with respect to the robot body (the point on the vertical line passing through the tire axles with respect to the top plate of a robot body) (C reference).

#### B. Conditional Expression for Gravitational Acceleration

In explaining the conditional expression related to gravitational acceleration, I first define the robot coordinate system and the piping coordinate system (right-hand Cartesian coordinate system). In the robot coordinate system, the center of the robot is the origin, the front of the robot is the positive direction of the  $x$ -axis, and the direction of gravity when the robot is placed on flat ground is the negative direction of the  $y$ -axis (Figure 3). In the absolute coordinate system, the pipe is placed on the  $x$ -axis so that the center of the pipe passes through the origin, and the pipe is installed with a gradient  $\theta_s$  rad with respect to the ground ( $x$ -axis). In other words, the pipe coordinate system is the absolute coordinate system rotated around the  $y$ -axis by the gradient  $\theta_s$  rad. Next, the gravitational acceleration will be described. The robot is equipped with an acceleration sensor, and the gravitational acceleration direction can be calculated from the sensor value (each component of the acceleration sensor) when the robot is stationary. Similarly, the robot posture (roll, pitch) in the pipe in the absolute coordinate system can be calculated using this sensor value (Equations (1) and (2)). Each variable is defined as follows.

${}^o\alpha_r$ : Rotation angle around the  $x$ -axis of the robot (roll) (absolute coordinate system) (rad)

${}^o\beta_r$ : Rotation angle around the  $y$ -axis of the robot (pitch) (absolute coordinate system) (rad)

${}^r a_x$ :  $x$ -component of the accelerometer (robot coordinate system) ( $m/s^2$ )

${}^r a_y$ :  $y$ -component of the accelerometer (robot coordinate system) ( $m/s^2$ )

${}^r a_z$ :  $z$ -component of the accelerometer (robot coordinate system) ( $m/s^2$ )

$${}^o\alpha_r = -\tan^{-1} \frac{{}^r a_y}{-{}^r a_z} \quad (1)$$

$${}^o\beta_r = -\tan^{-1} \frac{{}^r a_x}{-{}^r a_z} \quad (2)$$

#### C. Conditional Expression for Ground Contact Point of Tires

Three or more tires of the robot always touch the pipe as mentioned in the condition of III.A.1. Therefore, since the pipe becomes circular when viewed from the front, (3) holds at the grounding point according to Pythagorean theorem. Also, based on the condition of III.A.2,  ${}^s y_i$  and  ${}^s z_i$  can be expressed by (4). (4) finds the mounting position of each tire ( $[{}^o x_i \quad {}^o y_i \quad {}^o z_i]^T$ ) by adding the displacement to the mounting position of each tire to the position of the robot ( $[{}^o x_r \quad {}^o y_r \quad {}^o z_r]^T$ ) in the absolute coordinate system. At this time, the displacement of each tire to the mounting position in the absolute coordinate system is obtained by rotating the tire mounting position in the robot coordinate system by  ${}^o\alpha_r$  around the  $x$ -axis,  ${}^o\beta_r$  around the  $y$ -axis, and  ${}^o\gamma_r$  around the  $z$ -axis. Furthermore, (5) and (6) are obtained by substituting (4) for (3). Each variable is defined in as follows and in Figure 3.

${}^o x_r$ :  $x$ -component of the robot position (absolute coordinate system) (m)

${}^o y_r$ :  $y$ -component of the robot position (absolute coordinate system) (m)

${}^o z_r$ :  $z$ -component of the robot position (absolute coordinate system) (m)

${}^o\gamma_r$ : Rotation angle around the  $z$ -axis of the robot (yaw) (absolute coordinate system) (rad)

$i$  : Each wheel of the robot ( $fl, fr, br, bl$ )

$fl$  : The robot left front wheel

$fr$  : The robot right front wheel

$bl$  : The robot left rear wheel

$br$  : The robot right rear wheel

${}^o x_i$ : The robot tire mounting position ( $x$ -component) (absolute coordinate system) (m)

${}^o y_i$ : The robot tire mounting position ( $y$ -component) (absolute coordinate system) (m)

${}^o z_i$ : The robot tire mounting position ( $z$ -component) (absolute coordinate system) (m)

${}^s y_i$ : The robot tire mounting position ( $y$ -component) (pipe coordinate system) (m)

${}^s z_i$ : The robot tire mounting position ( $z$ -component) (pipe coordinate system) (m)

${}^r x_i$ : The robot tire mounting position ( $x$ -component) (robot coordinate system) (m)

${}^r y_i$ : The robot tire mounting position ( $y$ -component) (robot coordinate system) (m)

${}^r z_i$ : The robot tire mounting position ( $z$ -component) (robot coordinate system) (m)

${}^o p_i$ : Grounding position of the tires and the pipe (world coordinate system) (m)

$r_t$ : The tires radius (m)

$r_s$ : Inner radius of the pipe (m)

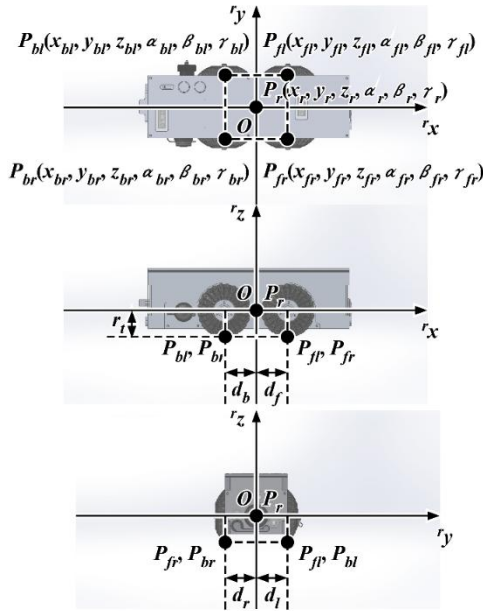


Fig. 3 Variables used for Localization

$$r_s^2 = s_y^2 + s_z^2 \quad (3)$$

$$\begin{aligned}
 {}^o\mathbf{p}_i &= \begin{bmatrix} {}^o x_i \\ {}^o y_i \\ {}^o z_i \end{bmatrix} \quad (i = fl, fr, bl, br) \\
 &= \begin{bmatrix} \cos {}^o\gamma_r & -\sin {}^o\gamma_r & 0 \\ \sin {}^o\gamma_r & \cos {}^o\gamma_r & 0 \\ 0 & 0 & 1 \end{bmatrix} \begin{bmatrix} r_x \\ r_y \\ r_z \end{bmatrix} + \begin{bmatrix} {}^o x_r \\ {}^o y_r \\ {}^o z_r \end{bmatrix} \\
 &= \begin{bmatrix} \cos {}^o\beta_r & 0 & \sin {}^o\beta_r \\ 0 & 1 & 0 \\ -\sin {}^o\beta_r & 0 & \cos {}^o\beta_r \end{bmatrix} \begin{bmatrix} 1 & 0 & 0 \\ 0 & \cos {}^o\alpha_r & -\sin {}^o\alpha_r \\ 0 & \sin {}^o\alpha_r & \cos {}^o\alpha_r \end{bmatrix} \begin{bmatrix} r_x \\ r_y \\ r_z \end{bmatrix} + \begin{bmatrix} {}^o x_r \\ {}^o y_r \\ {}^o z_r \end{bmatrix} \\
 &= \begin{bmatrix} r_x \cos {}^o\beta_r \cos {}^o\gamma_r \\ + r_y (\sin {}^o\alpha_r \sin {}^o\beta_r \cos {}^o\gamma_r \\ - \cos {}^o\alpha_r \sin {}^o\gamma_r) \\ + r_z (\cos {}^o\alpha_r \sin {}^o\beta_r \cos {}^o\gamma_r \\ + \sin {}^o\alpha_r \sin {}^o\gamma_r) + {}^o x_r \\ \\ r_x \cos {}^o\beta_r \sin {}^o\gamma_r \\ + r_y (\sin {}^o\alpha_r \sin {}^o\beta_r \sin {}^o\gamma_r \\ + \cos {}^o\alpha_r \cos {}^o\gamma_r) \\ + r_z (\cos {}^o\alpha_r \sin {}^o\beta_r \sin {}^o\gamma_r \\ - \sin {}^o\alpha_r \cos {}^o\gamma_r) + {}^o y_r \\ \\ - r_x \sin {}^o\beta_r \\ + r_y \sin {}^o\alpha_r \cos {}^o\beta_r \\ + r_z \cos {}^o\alpha_r \cos {}^o\beta_r + {}^o z_r \end{bmatrix} \quad (4)
 \end{aligned}$$

$$\begin{aligned}
 s_y &= (r_x \cos {}^o\beta_r + r_y \sin {}^o\alpha_r \sin {}^o\beta_r \\
 &+ r_z \cos {}^o\alpha_r \sin {}^o\beta_r) \sin {}^o\gamma_r \\
 &+ (r_y \cos {}^o\alpha_r - r_z \sin {}^o\alpha_r) \cos {}^o\gamma_r \\
 &+ {}^o y_r \quad (5)
 \end{aligned}$$

$$s_z = (r_y \cos {}^o\alpha_r \sin \theta_s$$

$$\begin{aligned}
 &- r_z \sin {}^o\alpha_r \sin \theta_s) \sin {}^o\gamma_r \\
 &+ (-r_x \cos {}^o\beta_r \sin \theta_s \\
 &- r_y \sin {}^o\alpha_r \sin {}^o\beta_r \sin \theta_s \\
 &- r_z \cos {}^o\alpha_r \sin {}^o\beta_r \sin \theta_s) \cos {}^o\gamma_r \\
 &+ (r_x \sin {}^o\beta_r \cos \theta_s \\
 &+ r_y \sin {}^o\alpha_r \cos {}^o\beta_r \cos \theta_s \\
 &+ r_z \cos {}^o\alpha_r \cos {}^o\beta_r \cos \theta_s) \\
 &+ {}^o z_r \cos \theta_s \quad (6)
 \end{aligned}$$

#### D. Handling x-component

${}^o x_r$  in (4) is the position of the robot in the pipe (distance traveled in the pipe) and is not directly related to the posture of the robot (roll). Therefore, it can be excluded as  ${}^o x_r = 0$ . As a result, the unknown variables in this localization are the five components  ${}^o y_r$ ,  ${}^o z_r$ ,  ${}^o\alpha_r$ ,  ${}^o\beta_r$ , and  ${}^o\gamma_r$ . It is assumed that  $r_s$  and  $\theta_s$  are known in advance.

#### E. Deriving Unknown Variables

As described in III.D, the unknown variables obtained by localization are the five components  ${}^o y_r$ ,  ${}^o z_r$ ,  ${}^o\alpha_r$ ,  ${}^o\beta_r$ , and  ${}^o\gamma_r$ .  ${}^o\alpha_r$  and  ${}^o\beta_r$  are obtained by substituting the sensor values of the accelerometer mounted on the robot into (1) and (2). Next, the obtained  ${}^o\alpha_r$  and  ${}^o\beta_r$  are substituted into (3), respectively. Furthermore, since three or four tires always touch the pipe under the conditions of III.A.1, three or four equations are obtained for (3). By eliminating  ${}^o y_r$  and  ${}^o z_r$  using three of these equations, they are converted into equations consisting only of  ${}^o\gamma_r$ . However, although this equation consists only of  ${}^o\gamma_r$ , the solution cannot be derived by the algebraic method. Therefore, numerical analysis is performed on  ${}^o\gamma_r$  in the range of  $\pm 30$  degree to find the solution of  ${}^o\gamma_r$  (see IV.C). Finally, by calculating back,  ${}^o y_r$  and  ${}^o z_r$  can also be obtained.

### IV. EXAMINATION OF LOCALIZATION BY EXPERIMENT

#### A. Measurement Method of Actual Measurement Value

Figure 4 shows the state of the verification experiment of localization. A 6-axis stage (a posture measuring device) with a jig and a scale were used to measure the actual measurement values, which are the comparison targets (Figure 5).

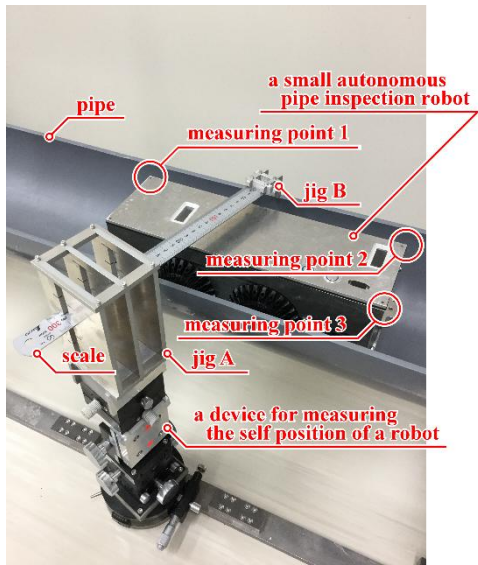


Fig. 4 Names of each instruments in verification experiments

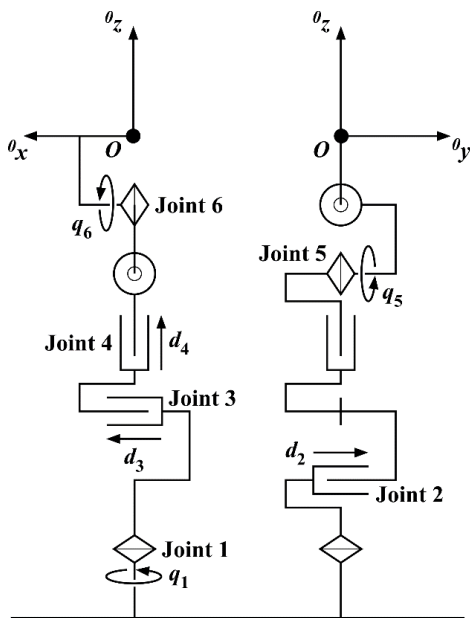


Fig. 5 Six-axis stage degrees of freedom

**B. Experiment Method**

The localization is performed according to the procedure described in III.E based on the sensor value (average value of 100 data) of the accelerometer obtained from the robot. In addition, the attaching error of the robot's acceleration sensor is calibrated in advance. Also, the number of experiments was 60 under the following conditions.

**Condition 1:** In the experiment, a pipe with an inner diameter of 189 mm was used, and the gradient was carried out in two patterns of 0.0 degree and approx. 2.4 degree (approx. 4/100).

**Condition 2:** The robot installed so that  $\theta_{\gamma_r}$  was approx. 3 to 4 degrees (Pattern 1), approx. 0 degree (Pattern 2), and approx. -4 to -3 degrees (Pattern 3), respectively.

**Condition 3:** Measurements were performed 10 times for each pattern under condition 2. In addition, the robot was re-installed in the pipe after each measurement (60 times).

**C. Results**

Figure 6 shows an example of the results of numerical analysis of  $\theta_{\gamma_r}$  within a range of  $\pm 30$  degree at 0.1 degree intervals. When numerical analysis is performed, three convergence points occur, as seen in the figure. The first point is the convergence point to infinity that occurs when the denominator approaches 0 infinitely, which can be ignored. The remaining two points represent the actual state (real image) where the robot is installed at the bottom of the pipe and the impossible state (virtual image) where the robot is installed at the ceiling of the pipe, as shown in Figure 7. The real image and the virtual image can be discriminated by the estimated value of  $\theta_{z_r}$ . In the case of the virtual image, the robot exceeds a certain reference value and floats in the air.

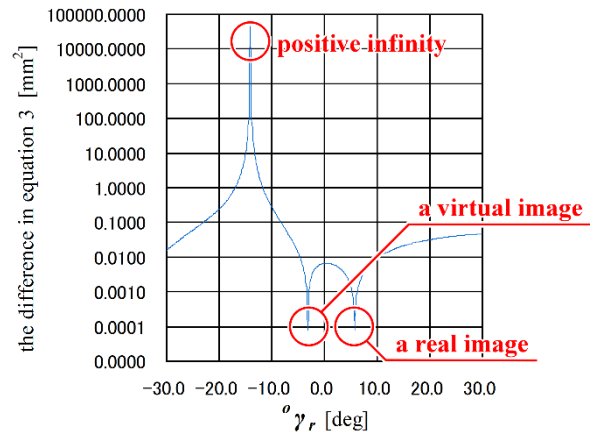


Fig. 6 Three convergence points

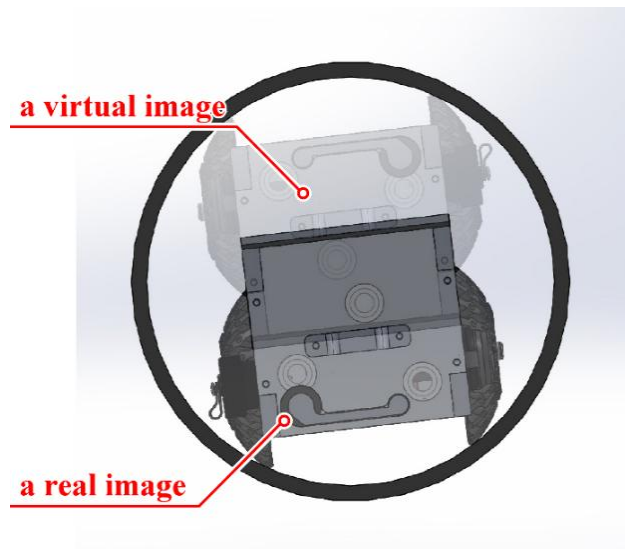


Fig. 7 Real image and virtual image

Next, the results of localization are shown in Figures 8, 9, Table I, and Table II. The graphs and Tables are for Fig. 8 and Table I when the pipe is not tilted (horizontal) and Fig. 9 and Table II when the pipe is tilted (gradient approx. 4/100). Table III shows the correspondence between the labels and variables in Fig. 8 and Fig. 9.



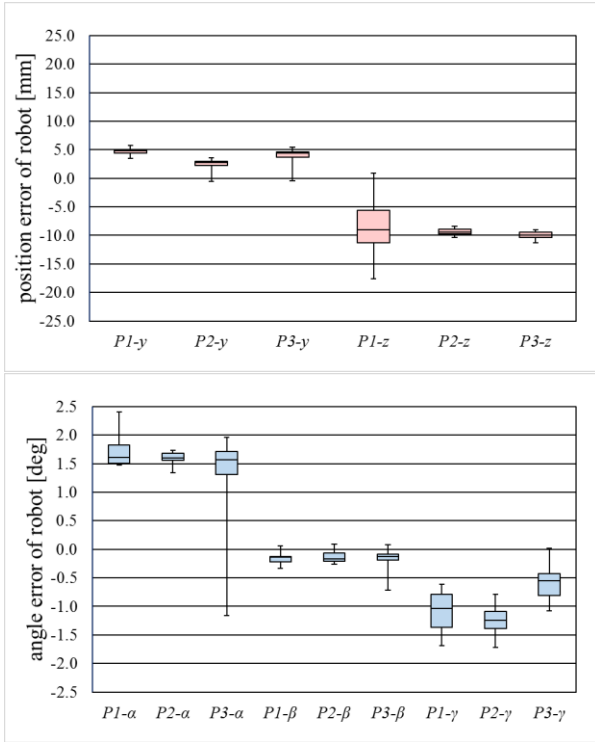


Fig. 8 Localization result without gradient

Table- I: Localization result without gradient

item		P1-y	P2-y	P3-y	P1-z	P2-z	P3-z
maximum - 75%		0.9	0.5	0.8	-6.3	-0.6	-0.9
75% - median		0.1	0.2	0.3	-2.3	-0.3	-0.4
median - 25%		0.4	0.5	0.7	-3.4	-0.5	-0.4
25%		4.4	2.3	3.6	-5.6	-8.9	-9.5
25% - minimum		0.9	2.8	4.1	-6.4	-0.5	-0.4

item	P1-α	P2-α	P3-α	P1-β	P2-β	P3-β	P1-γ	P2-γ	P3-γ
maximum - 75%	0.6	0.0	0.2	-0.1	0.0	-0.5	-0.3	-0.3	-0.3
75% - median	0.2	0.1	0.1	-0.1	0.0	-0.1	-0.3	-0.1	-0.3
median - 25%	0.1	0.0	0.3	0.0	-0.1	0.0	-0.2	-0.2	-0.1
25%	1.5	1.6	1.3	-0.1	-0.1	-0.1	-0.8	-1.1	-0.4
25% - minimum	0.0	0.2	2.5	-0.2	-0.2	-0.2	-0.2	-0.3	-0.4

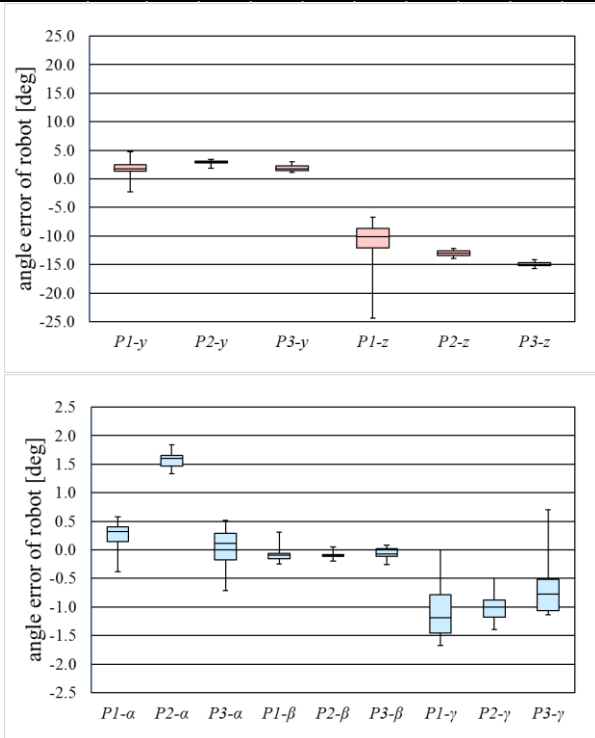


Fig. 9 Localization result with gradient

Table- II: Localization result with gradient

item		P1-y	P2-y	P3-y	P1-z	P2-z	P3-z
maximum - 75%		2.3	0.4	0.7	-12.3	-0.5	-0.5
75% - median		0.7	0.2	0.5	-2.0	-0.4	-0.2
median - 25%		0.4	0.1	0.3	-1.4	-0.4	-0.3
25%		1.3	2.7	1.4	-8.7	-12.6	-14.7
25% - minimum		3.6	0.9	0.3	-1.9	-0.4	-0.5

item	P1-α	P2-α	P3-α	P1-β	P2-β	P3-β	P1-γ	P2-γ	P3-γ
maximum - 75%	0.2	0.2	0.2	-0.1	-0.1	-0.1	-0.2	-0.2	-0.1
75% - median	0.1	0.1	0.2	-0.1	0.0	0.0	-0.3	-0.2	-0.3
median - 25%	0.2	0.1	0.1	0.0	0.0	-0.1	-0.4	-0.1	-0.3
25%	0.1	1.5	-0.2	-0.1	-0.1	0.0	-0.8	-0.9	-0.5
25% - minimum	0.5	0.1	0.5	-0.4	-0.1	-0.1	-0.8	-0.4	-1.2

Table- III: Relationship between labels and variables

label	variable	label	variable
P1-α	Pattern 1 ${}^o\alpha_r$	P1-y	Pattern 1 ${}^o\gamma_r$
P2-α	Pattern 2 ${}^o\alpha_r$	P2-y	Pattern 2 ${}^o\gamma_r$
P3-α	Pattern 3 ${}^o\alpha_r$	P3-y	Pattern 3 ${}^o\gamma_r$
P1-β	Pattern 1 ${}^o\beta_r$	P1-z	Pattern 1 ${}^o\zeta_r$
P2-β	Pattern 2 ${}^o\beta_r$	P2-z	Pattern 2 ${}^o\zeta_r$
P3-β	Pattern 3 ${}^o\beta_r$	P3-z	Pattern 3 ${}^o\zeta_r$
P1-γ	Pattern 1 ${}^o\gamma_r$		
P2-γ	Pattern 2 ${}^o\gamma_r$		
P3-γ	Pattern 3 ${}^o\gamma_r$		

Among these, there is an overall positive error for A. Since the attaching error of the robot's accelerometer was calibrated before the experiment, it is unlikely that this was the cause. On the other hand, since the rubber part of the tire used for the robot is made by the author, it is considered that the individual difference (shape and elasticity) of the tire itself is larger than that of other parts. Therefore, when the robot installed horizontally was measured by a calibrated level, it was found that the robot was slightly tilted to the right (gradient of 1/100 or less). This effect is also considered to appear in A and B. However, the posture error itself shows a constant value (offset), the swing width is small, and it is stable. Therefore, the method proposed in this paper is considered to be useful in posture estimation. In particular, since the error of A, which is important for the progress of the robot, is stable in the range of approx. -0.5 to -1.0 degrees, it is considered that the robot can withstand practicality sufficiently by correcting the error. On the other hand, a large error occurred in  ${}^o\zeta_r$ . It is probable that this is because the bowl-shaped tire was used for the robot in the evaluation experiment, and the pipe contacted the side surface of the tire instead of the bottom of the tire described in condition III.A.2. In fact, there is a stable and constant estimation error of approx. -10 mm, and the position 10 mm above the bottom of the tire is where the gripping force occur and is easy to touch the pipe due to the shape of the tire. In addition, the tires are provided with deep grooves in order to improve drainage, and the robot will sink further than usual when the grooves touch the pipe. It is newly found that this produces worse results for localization.

V. CONCLUSION

In this study, localization method using only accelerometer mounted on the robot, which focuses on the relation between the pipe and the contact point of the tires, was shown as well as presenting a method using numerical analysis to derive the estimated values.



Furthermore, it was confirmed that the estimation was stable as a result of an estimation experiment using autonomous small pipe inspection robot with and without a gradient (approx. 4/100) of a pipe, with a diameter of 189mm. Finally, through this experiment, two new issues were discovered.

### 1. Developing a stable robot that can localize itself

When a four-wheeled robot is used, the ground contact points are not stable at 2 to 4 points including vibration problem. Therefore, it is necessary to develop a three-wheeled robot for stable localization, and perform comparative verification with a four-wheeled robot.

### 2. Identifying the exact ground contact position between the tires and the pipe

In this study, because a bowl-shaped tire was used, it was clarified that the tires touch the pipe in a place different from the condition of III.A.2. For this reason, it is necessary to conduct experiments using tires of various shapes so that the localization method can be used with any robot, and to accurately identify the ground contact position between the tires and the pipe.

## REFERENCES

1. Japan institute of wastewater engineering technology, "Development foundation survey of sewerage facilities management robot", Sewer new technology Annual report of the Institute, 1992, pp.43-52.
2. Rome, E., Hertzberg, J., Kirchner, F., Licht, U. and Christaller, T., "Towards Autonomous Sewer Robots: the MAKRO Project", Urban Water, Vol. 1, 1999, pp. 57-70.
3. Streich, H. and Adria, O., "Software approach for the autonomous inspection robot MAKRO", in Proceedings of the 2004 IEEE International Conference Robotics and Automation, 2004, pp. 3411-3416.
4. Birkenhofer, C., Regenstein, K., Zöllner, J. M. and Dillmann, R., "Architecture of multi-segmented inspection Robot KAIRO-II", DOI: 10.1007/978-1-84628-974-3\_35, In book: Robot Motion and Control, 2007, pp.381-389.
5. Alireza, A., Yoshinori, K. and Masumi, I., "A laser scanner for landmark detection with the sewer inspection robot KANTARO", Proceedings of the IEEE International Conference on System of Systems Engineering, 2006, pp.310-315.
6. Alireza, A., Yoshinori, K. and Masumi, I., "An automated intelligent fault detection system for inspection of sewer pipes", IEEJ Transactions on Electronics, Information and Systems, Vol.127, No.6, 2007, pp.943-950.
7. Amir A. F. N., Yoshinori K., Alireza A., Yoshikazu M. and Kazuo I., "Concept and design of a fully autonomous sewer pipe inspection mobile robot "KANTARO"", IEEE International Conference on Robotics and Automation, 2007, pp.4088-4093.
8. Hirokazu, U. and Kazuo, I., "Basic research on crack detection for sewer pipe inspection robot using image processing", Proceedings of the 2009 JSME Conference on Robotics and Mechatronics, 2009, 1A1-C02.
9. Ryosuke, I., Yoshikazu, O., Shigeru, K., Yasuhiro, K., Yoshihiro, Y., Sakae, U., Takayuki, K., Hirofumi, M., Toshi, T. and Satoshi, T., "Development of remote control system for search and rescue robot in confined space", 2010 Symposium on System Integration, 2010, pp.1238-1241.
10. Hirofumi, M., Kiyoshi, I., Yoshikazu, O., Shigeru, K. and Toshi, T., "Development of Middleware for Rescue Robots to Facilitate Device Management", Proceedings of the JSME, No.115-1, 2011, p.123-124.
11. Hirofumi, M., Shigeru, K. and Toshi, T., "Development of system for rescue robots to facilitate device management", Bulletin of National Institute of Technology, Yuge College, Vol. 34, 2012, pp.48-53.
12. Ayaka, N., Kazutomo, F., Toshikazu, S., Mikio, G. and Hirofumi M., "Prototype design for a piping inspection robot", 43rd Graduation Research Presentation Lecture of Student Members of the JSME, 2013, 716.
13. Kazutomo, F., Yoshiki, I. and Hirofumi M., "Modularization for a piping inspection robot", 2013 Symposium on System Integration, 2013, pp.1297-1300.
14. Kazutomo, F., Toshikazu, S., Mikio, G., Yoshiki, I. and Hirofumi M., "Miniaturization of the piping inspection robot by modularization", 44rd

Graduation Research Presentation Lecture of Student Members of the JSME, 2014, 613.

15. Hirofumi, M., Takuya, K., Kazutomo, F., Yoshiki, I., Toshikazu, S. and Mikio, G., "Research and development about a piping inspection robot - Report1: Prototype design for a miniaturization -", Bulletin of National Institute of Technology, Yuge College, Vol. 36, 2014, pp.79-82.
16. Hirofumi, M., Yoshiki, I., Toshikazu, S. and Mikio, G., "Research and development about a piping inspection robot - Report2: Prototype design for maintenance improvement -", Bulletin of National Institute of Technology, Yuge College, Vol. 37, 2015, pp.75-79.
17. Hirofumi M., Ryota, K., "Development of a small autonomous pipe inspection robot (Modularization of hardware using the technique of wooden mosaic work)", Transactions of the Japan Society of Mechanical Engineers, Vol.82, No.839, 2016, pp.1-16.

## AUTHOR PROFILE



**Hirofumi Maeda** is Associate Professor in the Information Science and Technology Department at National Institute of Technology (KOSEN), Yuge College. Dr. Maeda's research focuses on practical application of mechanical engineering, namely, developing rescue robots, pipe inspection robots and natural language processing. Dr. Maeda previously served as a researcher at the NPO International Rescue System Institute. Dr. Maeda is currently a member of the Japan Society of Mechanical Engineers, the Robotics Society of Japan, the Japan Association for College of Technology, and the Japan Institute of Marine Engineering. Dr. Maeda has published eight peer-reviewed papers and presented 77 papers. In addition, Dr. Maeda received two awards at academic conferences and 12 external funds.